

1 **Preventive efficacy of a tenofovir alafenamide fumarate nanofluidic implant in SHIV-**
2 **challenged nonhuman primates**

3
4 **Authors:** Fernanda P. Pons-Fauoa^{1,2}, Antons Sizovs¹, Kathryn A. Shelton³, Zoha Momin⁴,
5 Lane R. Bushman⁵, Jiaqiong Xu^{6,7}, Corrine Ying Xuan Chua¹, Joan E. Nichols⁸, Trevor
6 Hawkins⁹, James F. Rooney⁹, Mark A. Marzinke¹⁰, Jason T. Kimata⁴, Peter L. Anderson⁵,
7 Pramod N. Nehete^{3,11}, Roberto C. Arduino¹², Mauro Ferrari¹³, K. Jagannadha Sastry^{3,14},
8 Alessandro Grattoni^{1,15,16*}

9
10 **Affiliations:**

11 ¹Department of Nanomedicine, Houston Methodist Research Institute, Houston, TX 77030, USA

12 ²Tecnologico de Monterrey, School of Medicine and Health Sciences, Monterrey, NL, Mexico

13 ³Department of Comparative Medicine, Michael E. Keeling Center for Comparative Medicine
14 and Research, MD Anderson Cancer Center, Bastrop, TX 78602, USA

15 ⁴Department of Molecular Virology and Microbiology, Baylor College of Medicine, Houston,
16 TX 77030, USA

17 ⁵Department of Pharmaceutical Sciences, Skaggs School of Pharmacy and Pharmaceutical
18 Sciences, University of Colorado- Anschutz Medical Campus, Aurora, CO 80045, USA

19 ⁶Center for Outcomes Research and DeBakey Heart and Vascular Center, Houston Methodist
20 Research Institute, Houston, TX 77030, USA

21 ⁷Weill Medical College of Cornell University, New York, NY 10065, USA

22 ⁸Division of Infectious Diseases, Department of Internal Medicine, University of Texas Medical
23 Branch (UTMB), Galveston, TX 77555, USA

24 ⁹Gilead Sciences, Inc., Foster City, CA 94404, USA

25 ¹⁰Departments of Pathology and Medicine, Johns Hopkins University School of Medicine,
26 Baltimore, MD 21224, USA

27 ¹¹The University of Texas Graduate School of Biomedical Sciences at Houston, Houston, TX
28 77030, USA

29 ¹²Division of Infectious Diseases, Department of Internal Medicine, McGovern Medical School
30 at The University of Texas Health Science Center, Houston, TX 77030, USA

31 ¹³School of Pharmacy, University of Washington, Seattle, WA 98195, USA

32 ¹⁴Department of Thoracic Head and Neck Medical Oncology, University of Texas MD Anderson
33 Cancer Center, Houston, TX 77030, USA

34 ¹⁵Department of Surgery, Houston Methodist Research Institute, Houston, TX 77030, USA

35 ¹⁶Department of Radiation Oncology, Houston Methodist Research Institute, Houston, TX
36 77030, USA

37 *Corresponding author: Alessandro Grattoni, email: agrattoni@houstonmethodist.org

38

39 **Keywords:** Nanofluidics, HIV pre-exposure prophylaxis, tenofovir alafenamide, implantable
40 devices, drug delivery

41

42 **Abstract**

43 Pre-exposure prophylaxis (PrEP) using antiretroviral oral drugs is effective at preventing HIV
44 transmission when individuals adhere to the dosing regimen. Tenofovir alafenamide (TAF) is a
45 potent antiretroviral drug, with numerous long-acting (LA) delivery systems under development
46 to improve PrEP adherence. However, none has undergone preventive efficacy assessment. Here

47 we show that LA TAF using a novel subcutaneous nanofluidic implant (nTAF) confers partial
48 protection from HIV transmission. We demonstrate that sustained subcutaneous delivery through
49 nTAF in rhesus macaques maintained tenofovir diphosphate concentration at a median of 390.00
50 fmol/10⁶ peripheral blood mononuclear cells, 9 times above clinically protective levels. In a non-
51 blinded, placebo-controlled rhesus macaque study with repeated low-dose rectal SHIV_{SF162P3}
52 challenge, the nTAF cohort had a 62.50% reduction (95% CI: 1.72% to 85.69%; *p*=0.068) in risk
53 of infection per exposure compared to the control. Our finding mirrors that of tenofovir
54 disoproxil fumarate (TDF) monotherapy, where 60.00% protective efficacy was observed in
55 macaques, and clinically, 67.00% reduction in risk with 86.00% preventive efficacy in
56 individuals with detectable drug in the plasma. Overall, our nanofluidic technology shows
57 potential as a subcutaneous delivery platform for long-term PrEP and provides insights for
58 clinical implementation of LA TAF for HIV prevention.

59

60 **1. Introduction**

61 The approval of Descovy® (200 mg emtricitabine [FTC]/25 mg tenofovir alafenamide [TAF]) as
62 the second HIV pre-exposure prophylaxis (PrEP) medication, following Truvada® (200 mg
63 FTC/300 mg tenofovir disoproxil fumarate [TDF]) is fueling global efforts to end the AIDS
64 pandemic by 2030.^[1] Compared to Truvada®, Descovy® offers safety advantages with lower
65 systemic tenofovir (TFV) concentrations without compromising overall efficacy
66 (NCT02842086).^[2] The efficacy of these agents to prevent sexual HIV infection is exceptional,
67 provided that individuals strictly adhere to the dosing regimen.^[3-5] According to the iPrEx study,
68 seven doses of Truvada® per week correlated with 99% PrEP efficacy, whereas the rate dropped
69 to 76% with two doses per week.^[6] Motivated by challenges of pill fatigue and PrEP

70 accessibility, various biomedical developments have emerged aiming at improving therapeutic
71 adherence and expanding HIV PrEP implementation.
72
73 Long-acting (LA) antiretroviral (ARV) formulations and delivery systems offer systemic
74 delivery for prolonged periods, obviating the need for frequent dosing. Currently, LA ARV
75 strategies for HIV PrEP are largely geared towards developing single-agent drugs for prevention
76 instead of combinatorial formulations.^[7-15] Focusing on a single drug allows for maximal drug
77 loading, while minimizing injection volumes (for injectables). In the case of LA ARV implants,
78 a single drug formulation affords smaller size dimensions for minimally-invasive and discreet
79 implantation.^[16,17] Importantly, single-agent LA ARVs offer benefits of cost-effectiveness as
80 well as reduced complexity in terms of development. Of relevance, a single-agent injectable LA
81 ARV, cabotegravir, is currently in clinical trials for PrEP efficacy evaluation (NCT02076178,
82 NCT02178800, NCT02720094, NCT03164564).^[18,19] Thus far, islatravir (MK-8591) remains the
83 only single-agent ARV LA ARV implant to reach clinical testing for safety and
84 pharmacokinetics assessment.^[20]
85
86 Given the potency and safety advantages of TAF compared to TDF, numerous LA TAF
87 strategies are under development involving biodegradable^[7-9] or non-biodegradable^[10] polymeric
88 implants, transcutaneously refillable devices^[11], and an osmotic pump system.^[15] While some LA
89 TAF systems have achieved targeted preventive tenofovir diphosphate (TFV-DP) concentrations
90 in peripheral blood mononuclear cells (PBMC) (40.0 fmol/10⁶ cells)^[7,10,11], none has undergone
91 efficacy studies for protection from HIV transmission. Thus, considering the concentrated

92 research efforts on developing LA TAF systems, it is of utmost importance to evaluate the
93 efficacy of LA TAF as a single-agent drug for HIV prevention.

94
95 Here, we present the first efficacy study of LA TAF for HIV PrEP. We used a nonhuman primate
96 (NHP) model of repeated low-dose rectal challenge with simian HIV_{SF162P3} (SHIV_{SF162P3}), which
97 recapitulates human HIV transmission. We assessed the efficacy of sustained subcutaneous
98 delivery of TAF via a novel nanofluidic (nTAF) implant as a single-agent PrEP regimen for
99 protection from SHIV_{SF162P3} infection. We investigated the pharmacokinetics and biodistribution
100 of TAF, as well as safety and tolerability of the implant.

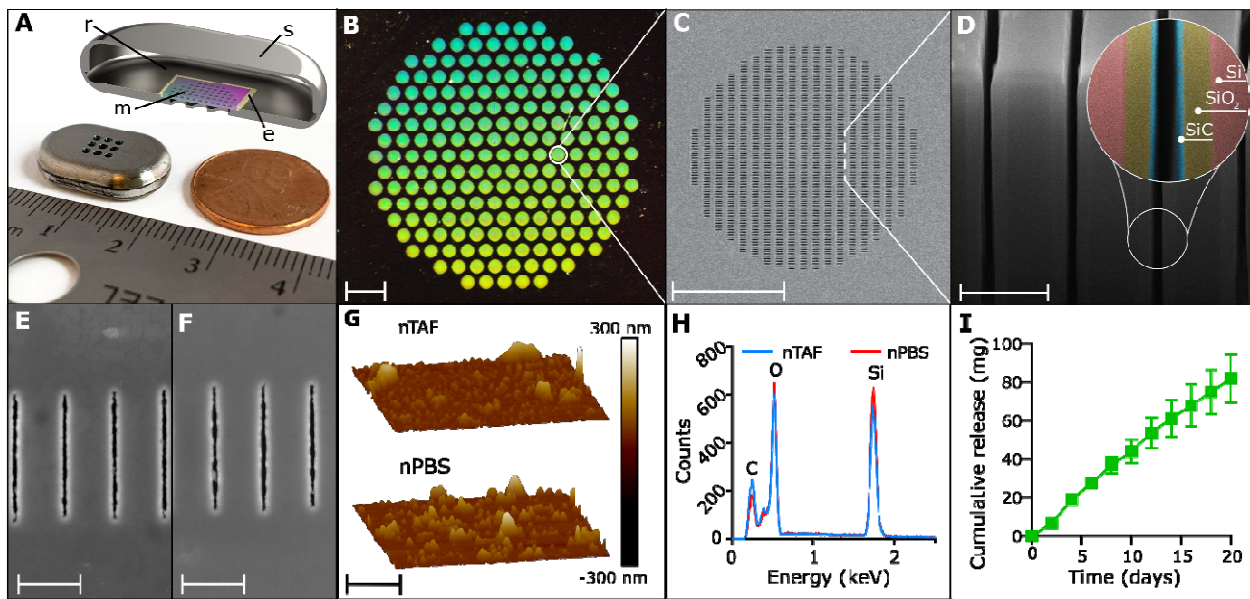
101

102 **2. Results**

103 **2.1. Nanofluidic implant assembly**

104 We leveraged a newly designed silicon nanofluidic membrane technology^[21] for sustained drug
105 elution independent of actuation or pumps. The nanofluidic membrane (6 mm × 6 mm with a
106 height of 500 μm) is mounted within a medical-grade titanium drug reservoir (**Figure 1A**). The
107 nanofluidic membrane contains 199 circular microchannels, each measuring 200 μm in diameter
108 and 490 μm in length. Hexagonally distributed in a circular configuration (Figure 1B), each
109 microchannel leads to 1400 parallel slit-nanochannels (Figure 1C), for a total of 278,600
110 nanochannels per membrane. The nanochannels (length 10 μm, width 6 μm) are densely packed
111 in square arrays organized in circular patterns. The whole membrane surface is coated by an
112 innermost layer consisting of silicon dioxide (SiO₂), and a surface layer of silicon carbide (SiC),
113 which provides biochemical inertness for long term implantable applications (Figure 1D).^[22,23]

114



115
116 **Figure 1.** The nanofluidic implant for subcutaneous TAF HIV PrEP delivery. A) Rendered
117 image of cross-section of titanium drug reservoir. B) Assembled titanium TAF drug reservoir
118 with 200 nm nanofluidic membrane. Image taken at 0.5 x magnification, scale bar is 1 mm. C)
119 Top-view of SEM image of nanochannel membrane. Scale bar is 100 μm. D) FIB image of
120 nanochannel membrane cross-section displaying perpendicular nanochannels. Zoom-in on
121 nanochannel layers colored for identification. Scale bar is 2 μm. E) Representative top view
122 SEM image of nanochannel membrane from nTAF after 4 months in vivo. Scale bar is 2.5 μm.
123 F) Representative top view SEM image of nanochannel membrane from nPBS after 4 months in
124 vivo. Scale bar is 2.5 μm. G) Representative AFM image of membrane from nTAF compared to
125 AFM image of membrane from nPBS after 4 months in vivo. Scale bar is 2.5 μm. H) EDX
126 analysis of surface elements below SiC coating of membrane from nTAF compared to nPBS
127 after 4 months in vivo. I) Cumulative release of drug *in vitro* (mean ± SEM) from nTAF into
128 sink solution (n=5). SiC, silicon carbide, SiO₂, silicon oxide, Si, silicon.
129

130 Drug diffusion across the membrane is driven by concentration difference between the drug
131 reservoir and the subcutaneous space. The drug is loaded in the implant in powder form and is
132 continuously solubilized in the interstitial fluids penetrated within the implant via capillary
133 wetting of the membrane. Drug release is determined by both nanochannels and drug
134 solubilization kinetics. Within the nanochannels, diffusivity of drug molecules is defined by
135 steric and electrostatic interactions with channel walls. The size of nanochannels is selected to
136 saturate drug transport, rendering it steady and independent from the concentration gradient.^[24,25]

137 The release rate can be finely tuned by selecting the suitable number of nanochannels per
138 membrane.^[26] Therefore, the nanofluidic membrane passively achieves constant and sustained
139 drug delivery obviating the need of mechanical components.^[27,28]

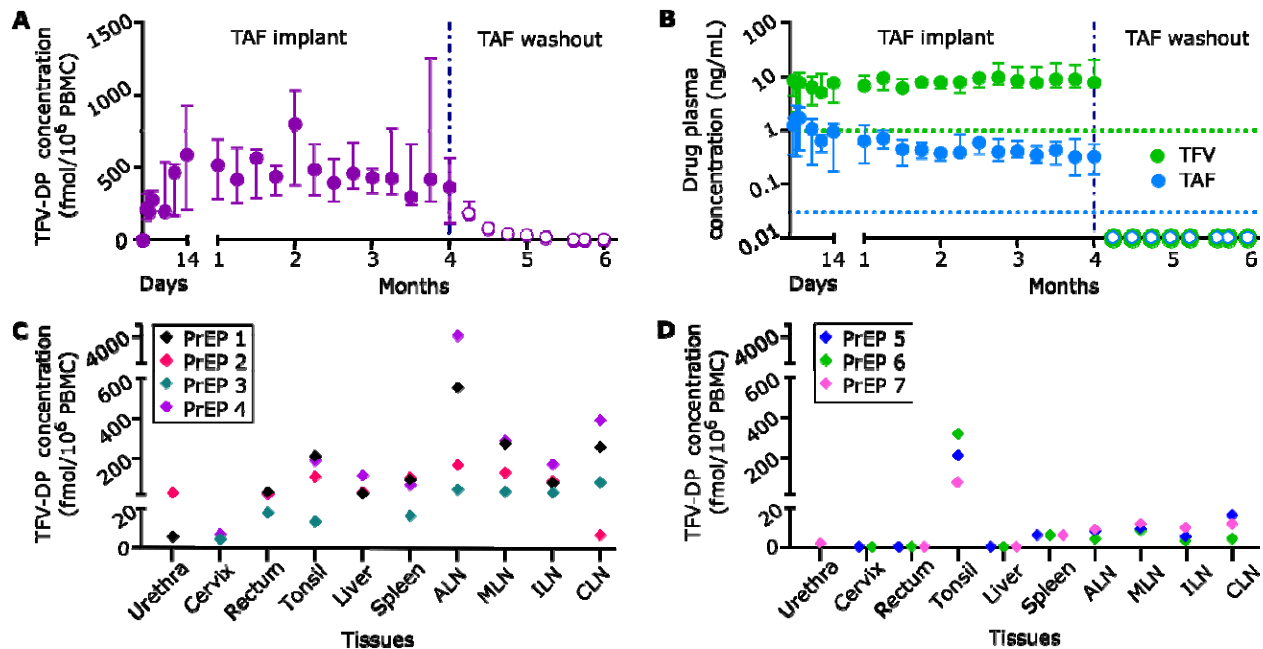
140
141 In this study, based on the molecular size and physicochemical properties of TAF, we used the
142 nanochannels size of ~190 nm. PrEP implants were loaded with solid powder TAF (nTAF),
143 while control implants were loaded with phosphate buffered saline (nPBS). Membrane stability
144 was evaluated after 4 months of subcutaneous implantation via scanning electron microscopy
145 (SEM) (Figure 1E and F) along with atomic force microscopy (AFM) (Figure 1G) and energy
146 dispersive x-ray spectroscopy (EDX) (Figure 1H). We observed similar surface morphology by
147 AFM for the nTAF and nPBS membranes, with a non-statistically significant increase in
148 roughness in the nPBS membrane. The EDX showed the same abundance of elements at the
149 surface in both membranes, indicating that TAF does not alter the membrane composition. These
150 results demonstrate that TAF does not affect membrane stability even after prolonged
151 implantation.

152
153 Short-term *in vitro* drug release from nTAF showed a linear cumulative release of 81.85 ± 12.55
154 mg (mean \pm SEM) of TAF over 20 days (Figure 1I). However, an increase of TAF degradation
155 products was observed throughout the study, attributable to decrease in TAF stability (Figure S1,
156 Supporting Information).

157

158 **2.2. nTAF pharmacokinetic profile in NHP**

159 For *in vivo* evaluation of pharmacokinetic (PK) and PrEP efficacy, rhesus macaques were
160 subcutaneously implanted with either nTAF (n=8) or control nPBS (n=6) in the dorsum for 4
161 months. We used TFV-DP concentration in PBMC of 100.00 fmol/10⁶ cells as the benchmark
162 prevention target, which exceeds the clinically protective level in the iPrEX trial.^[6,7] Preventive
163 TFV-DP PBMC concentrations were surpassed one day post-implantation (median, 213.00
164 fmol/10⁶ cells; IQR, 140.00 to 314.00 fmol/10⁶ cells) and maintained at a median of 390.00
165 fmol/10⁶ cells (IQR, 216.50 to 585.50 fmol/10⁶ cells) for 4 months (Figure 2A). During the
166 washout period, TFV-DP PBMC concentrations decreased to below the limit of quantitation
167 (BLOQ) within 6 weeks of device retrieval.
168



169
170 **Figure 2.** Pharmacokinetics and tissue distribution of TAF from PrEP group implanted with
171 subcutaneous nTAF. nTAF implants (n=7) were retrieved after 4 months and washout
172 concentrations (open circles) were followed in 3 animals. A) Intracellular TFV-DP PBMC
173 concentrations of PrEP cohort throughout the study. B) TAF and TFV concentrations in the
174 plasma of PrEP cohort throughout the study. Green and blue dotted horizontal lines represent
175 lower LOQ TFV and TAF concentrations, 1.00 ng/mL and 0.03 ng/mL, respectively. C) Tissue
176 TFV-DP concentrations upon nTAF removal after 4 months of implantation in a subset of
177 animals (n=4). D) Tissue TFV-DP levels after the 2-month washout period in a subset of animals
178 (n=3). Data are presented as median \pm IQR in panels A and B.

179
180 Plasma TFV concentrations were consistently higher than plasma TAF for the duration of the PK
181 study (Figure 2B). Notably, TFV concentrations increased as TAF concentrations decreased,
182 beginning at the 3-month time point. This is attributable to the limited stability of TAF and
183 degradation to TFV within the implant, as was observed *in vitro* (Figure S1, Supporting
184 Information).^[29] Plasma TAF and TFV levels (median, 0.51; IQR, 0.30 to 0.91 ng/mL; and
185 median, 7.81; IQR, 6.17 to 9.97 ng/mL, respectively) were within range of that achieved with
186 oral TAF dosing of NHP.^[30] Within a week post-device retrieval, TAF and TFV concentrations
187 were BLOQ.

188
189 Estimated half-life ($t_{1/2}$) PK of TAF and TFV were below 1.87 ± 0.32 and 1.84 ± 0.63 days,
190 respectively, as BLOQ was achieved in under a week (Table 1). Individual TFV-DP
191 concentrations for each animal were fitted to an intravenous bolus injection two-compartment
192 model (Figure S2A-D, Supporting Information). During the washout period, TFV-DP PBMC
193 concentrations had an average first-order elimination rate constant of 0.14 ± 0.028 days⁻¹.

194

Analyte	NHP PrEP 5	NHP PrEP 6	NHP PrEP 7	Average	Standard deviation
Plasma TAF $t_{1/2}$ (days)	<2.24	<1.71	<1.67	<1.87	± 0.32
Plasma TFV $t_{1/2}$ (days)	<2.55	<1.61	<1.35	<1.84	± 0.63
PBMC TFV-DP k ₁₀ (1/day)	0.18	0.13	0.13	0.14	± 0.028

195 **Table 1.** Plasma TAF and TFV half-lives and PBMC TFV-DP elimination rate constant
196 pharmacokinetics in nTAF washout NHPs.

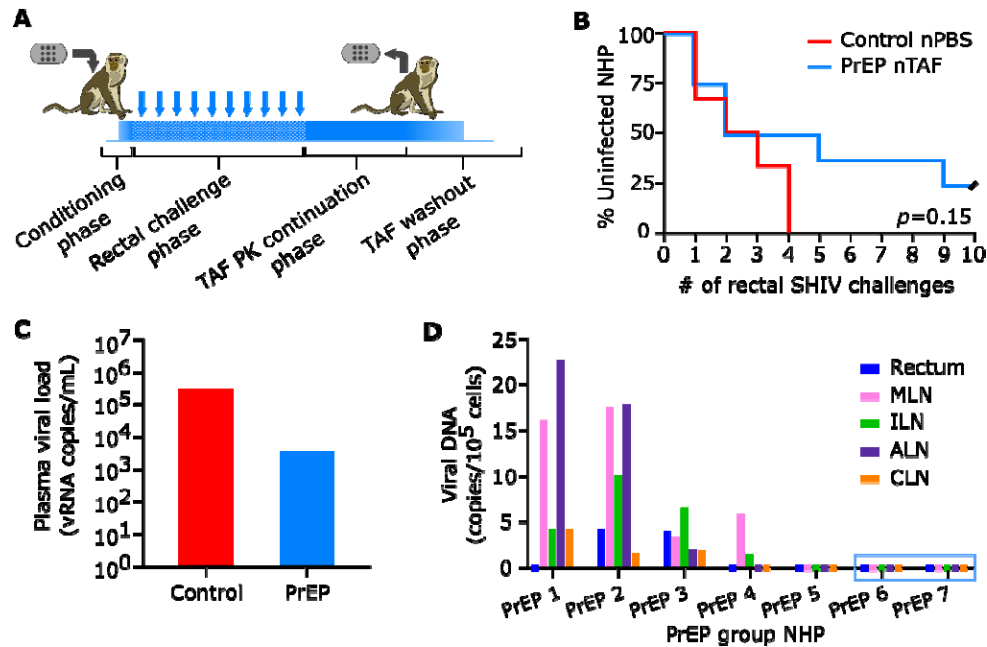
197

198 We measured TFV-DP concentrations after device retrieval (n=4) (Figure 2C) and after the
199 washout period (n=3) (Figure 2D) in tissues relevant to HIV-1 transmission or viral reservoirs.
200 Specifically, we assessed cervix, urethra, rectum, tonsil, liver, spleen, axillary lymph nodes
201 (ALN), mesenteric lymph nodes (MLN), inguinal lymph nodes (ILN), and cervical lymph nodes
202 (CLN). Drug penetration from subcutaneous TAF delivery was observed at varying levels in all
203 tissues after device retrieval (Figure 2C). After the two-month washout period, TFV-DP
204 concentrations were quantifiable in the tonsil, spleen and lymph nodes (Figure 2D) and BLOQ in
205 tissues highly associated with HIV-1 transmission, specifically the cervix and rectum. TFV-DP
206 concentrations in the tonsil were above 75.00 fmol/mg, suggestive of longer clearance or better
207 penetration.

208

209 **2.3. nTAF efficacy protection against virus**

210 We next assessed whether sustained nTAF delivery as a subcutaneously delivered monotherapy
211 could protect the macaques against rectal SHIV_{SF162P3} infection. Prior to rectal challenge, the
212 animals were subjected to a two-week “conditioning phase” (Figure 3A) to allow for reaching
213 the target preventive intracellular TFV-DP PBMC concentrations of 100.00 fmol/10⁶ cells
214 (Figure 2A). Animals in both PrEP (n=8) and control (n=6) cohorts were rectally challenged
215 weekly with low-dose SHIV_{SF162P3} for up to 10 inoculations and continually monitored for drug
216 PK throughout the study (Figure 3A). The SHIV inoculation dosage used are similar to human
217 semen HIV RNA levels during acute viremia, thus recapitulating high-risk or acute HIV
218 infection in humans. Therefore, this animal model is considered more aggressive, as the risk of
219 infection per exposure markedly exceeds the risk in clinical settings.^[31]



220
 221 **Figure 3.** PrEP efficacy of nTAF. A) Schematic of study design. Conditioning phase to reach
 222 TFV-DP PBMC concentrations above 100 fmol/10⁶ cells. Rectal challenge phase with up to 10
 223 weekly low-dose SHIV_{SF162P3} exposures. TAF PK continuation phase followed by nTAF
 224 explanation from all animals and euthanasia of 4 animals. TAF washout was observed in the
 225 remaining 3 animals for 2 months prior to euthanasia. B) Kaplan-Meier curve representing the
 226 percentage of infected animals as a function of weekly SHIV exposure. PrEP (n=8) vs control
 227 (n=6) group; censored animals represented with black slash. Statistical analysis by Mantel-Cox
 228 test. C) Median peak viremia levels in breakthrough animals at initial viral load detection. D)
 229 Cell-associated viral DNA loads of tissues in PrEP group. Animals PrEP 1-5 were infected while
 230 PrEP 6 and 7 (blue box) remained uninfected throughout the study. MLN, mesenteric lymph
 231 nodes, ILN, inguinal lymph nodes, ALN, axillary lymph nodes, CLN, cervical lymph nodes.
 232

233 To monitor for SHIV_{SF162P3} infection, we evaluated weekly cell-free viral RNA in the plasma.
 234 Rectal challenges were stopped upon initial detection of plasma viral RNA, which was
 235 confirmed after a consecutive positive assay. Two of eight macaques from the nTAF group
 236 (25.00%) were uninfected after 10 weekly rectal SHIV_{SF162P3} challenges (Figure 3B). Based on
 237 the number of infections per total number of challenges, the nTAF group had a reduced risk of
 238 infection per-exposure of 62.50% (95% CI, 1.72% to 85.69%; $p=0.068$), in comparison to the
 239 control group. However, because of the small sample size, the result is not very precise, as
 240 indicated by the lower bound of the confidence interval. Prophylaxis with nTAF increased the

241 median time to infection to 5 challenges compared to 2 challenges in the control cohort ($p=0.38$).
242 After device explantation, there was no spike in viremia, indicative of PrEP efficacy of nTAF
243 monotherapy in the two uninfected animals. While Kaplan-Meier analysis demonstrated delayed
244 and reduced infection in some animals, there was no statistical significance ($p=0.15$) between
245 nTAF and nPBS groups.

246

247 TAF-treated infected NHPs had blunted SHIV RNA peak viremia (median; 3.80×10^4 vRNA
248 copies/mL; IQR, 1.60×10^3 to 2.09×10^5 vRNA copies/mL) in comparison to control groups
249 (median; 3.01×10^5 vRNA copies/mL; IQR, 9.00×10^3 to 7.25×10^6 vRNA copies/mL) (Figure
250 3C). However, differences in SHIV RNA levels at initial detection were not statistically
251 significant between control and infected PrEP animals ($p=0.18$ by Mann-Whitney test).

252

253 At euthanasia, we assessed the residual SHIV infection in various tissues collected from the
254 nTAF cohort by measuring cell-associated SHIV_{SF162P3} provirus DNA (Figure 3D). Tissues from
255 PrEP 1-4 were assessed after 4 months of nTAF implantation, and after 2 months of drug
256 washout for PrEP 5-7. SHIV DNA was detectable in the MLN in 4/5 of the infected PrEP NHPs.
257 Animals PrEP 5 (infected) and PrEP 6 and 7 (uninfected), had no detectable SHIV DNA in any
258 of the tissues analyzed.

259

260 **2.4. Drug stability in vivo within nTAF**

261 To evaluate drug stability in nTAF after 4 months of *in vivo* implantation, we extracted residual
262 contents from the implant and analyzed for TAF and its hydrolysis products (TAF*) (Table 2).
263 Residual drug within the implant ranged 30.75 – 71.12% of the initial loaded amount. Further,

264 TAF* within the implant was predominantly composed of TAF hydrolysis products, including
265 TFV, with TAF stability ranging 18.21 - 43.08%. Therefore, augmented TAF hydrolysis to TFV
266 within the implant most likely contributed to increased TFV levels observed in plasma towards
267 the end of the study. The nTAF implants had a mean release rate of 1.40 ± 0.39 mg/day, which
268 was sufficient to sustain intracellular TFV-DP concentrations above 100.00 fmol/ 10^6 PBMCs
269 throughout the duration of the study.
270

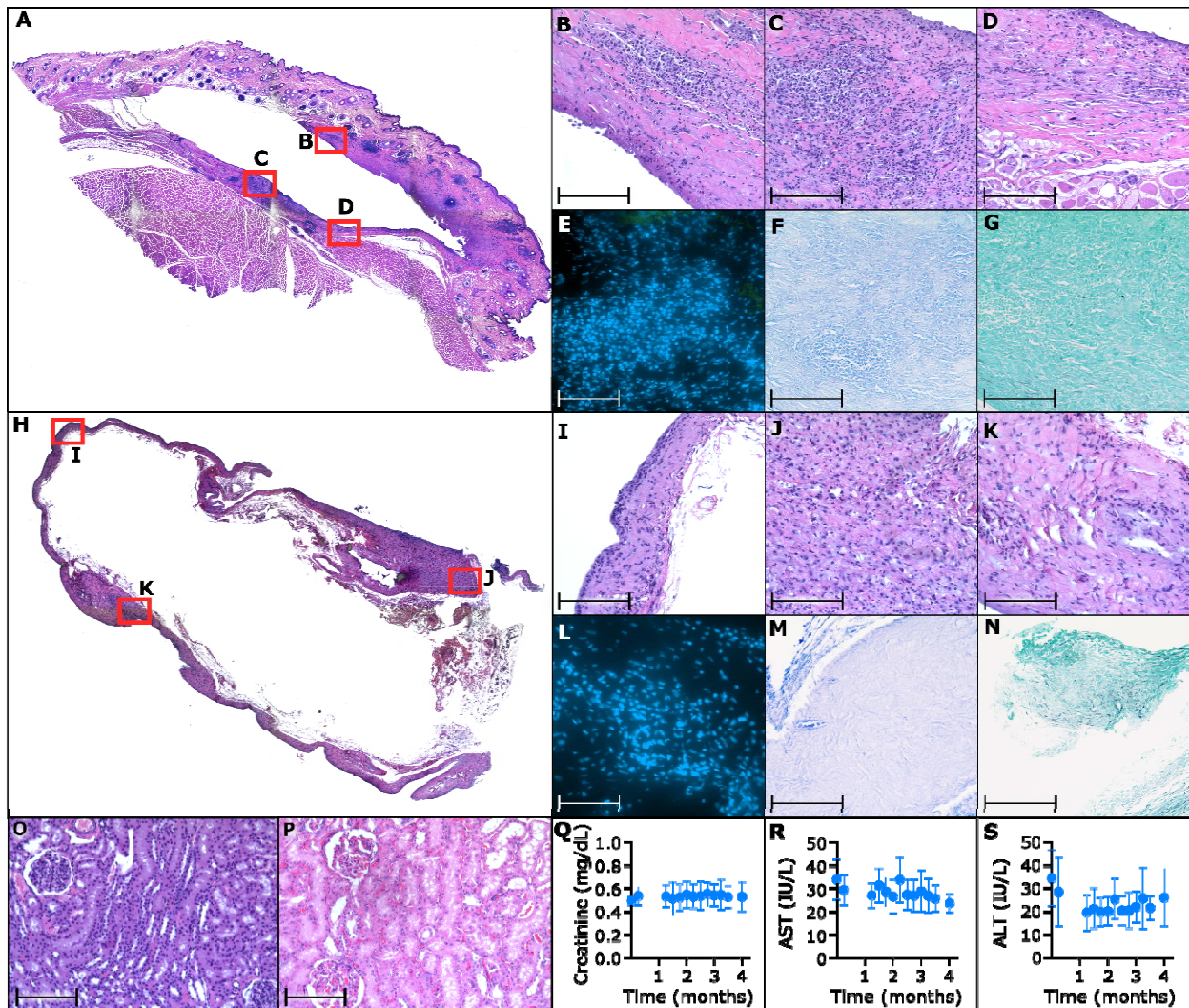
NHP PrEP	TAF loaded (mg)	Residual TAF* (mg)	TAF stability (%)	TAF release rate (mg/day)
1	341.50	161.87	30.76	1.60
2	330.10	217.65	12.28	1.00
3	337.10	215.57	18.21	1.09
4	382.10	241.01	31.78	1.26
5	457.60	325.43	43.08	1.18
6	449.30	279.46	18.70	1.52
7	342.60	105.34	22.26	2.12

271 **Table 2.** Residual drug analysis from nTAF implants at explantation via high performance liquid
272 chromatography (HPLC) and UV-Vis spectroscopy.
273

274 **2.5. nTAF safety and tolerability in NHP**

275 To assess nTAF safety and tolerability, we histologically examined the tissue surrounding the
276 implants after 4 months of implantation, through immunohistochemical analysis (Figure 4A).
277 Specifically, we evaluated the fibrotic capsule in contact with either the titanium reservoir
278 (Figure 4B) or TAF-eluting nanofluidic membrane (Figure 4C and D). Histological analysis via
279 hematoxylin and eosin (H&E) demonstrated foreign-body response, which is typical of medical
280 implants. The surrounding subcutaneous tissue and underlying skeletal muscle was healthy with

281 limited necrosis in the fibrotic capsule. While fibrotic capsules exhibited cellular infiltration,
282 they were negative for inflammatory cell marker CD45 (Figure 4E). DAPI staining demonstrated
283 healthy nuclei in the areas with increased cellular infiltration. Further, analysis of the fibrotic
284 area in contact with TAF-releasing membrane via acid-fast bacteria (AFB) (Figure 4F) and
285 Grocott methenamine silver staining (Figure 4G), which evaluates for presence of bacteria and
286 fungi, respectively, were negative.



287
288 **Figure 4.** Histological inflammatory response to nTAF and control nPBS; and toxicology
289 assessment of nTAF in the kidney and liver. A) Representative H&E stain of NHP skin
290 surrounding PrEP nTAF, with B) fibrotic capsule in contact with titanium implant; 20 ×
291 magnification. Fibrotic capsule in contact with TAF-releasing membrane was assessed via C), D)
292 H&E, 20 × magnification; E) immunofluorescence staining of CD45 (green) and DAPI nuclear
293 stain (blue), 100 × magnification; F) AFB staining for presence of bacteria, 20 × magnification;

294 and G) Grocott methenamine silver staining for presence of fungi, 20 × magnification. H)
295 Representative H&E stain of NHP skin surrounding control nPBS. Fibrotic capsule in contact
296 with titanium implant was assessed via I), J), K) H&E, 20 × magnification, L)
297 immunofluorescence staining of CD45 (green) and DAPI nuclear stain (blue), 100 ×
298 magnification; M) AFB staining for presence of bacteria, 20 × magnification; and N) Grocott
299 methenamine silver staining for presence of fungi, 20 × magnification. O) Representative H&E
300 stain of kidney from PrEP nTAF group demonstrating normal histology, in comparison to P)
301 representative H&E stain of kidney from control NHP similarly showing no nephrotoxicity; 20 ×
302 magnification. Q) Creatinine activity measurements from nTAF cohort. Liver enzymes, R)
303 aspartate aminotransferase (AST), and S) alanine aminotransferase (ALT) from nTAF cohort.
304 Baseline levels (0 month) were measured before implantation of nTAF. All data are presented as
305 mean ± SD (n=7). Images A and H taken at 4 × magnification and stitched together. Scale bar in
306 20 and 100 × magnification is 200 and 10 μm, respectively.
307

308 In parallel, as a control, the tissue surrounding nPBS implants were histologically assessed
309 (Figure 4H), specifically the fibrotic capsule (Figure 4I-K), which was thinner and denser than
310 the nTAF. Similarly, the tissue surrounding the control implant was negative for CD45 cells
311 (Figure 4L), bacteria (Figure 4M) or fungi (Figure 4N). While other groups have reported that
312 TAF induced necrosis at sites of implantation^[10], overall our results showed no cellular damage
313 or aberrant inflammatory cell influx, indicative of implant tolerability.

314
315 As TFV is implicated in nephrotoxicity and hepatotoxicity, we evaluated the kidney and liver in
316 the animals with nTAF implants. The kidney of an untreated NHP from a prior study was used as
317 a historical control, because nPBS NHPs were transferred to another study after infection.
318 Histological assessment of the kidney from nTAF cohort via H&E analysis (Figure 4O) did not
319 demonstrate necrosis or signs of damage, in comparison to control (Figure 4P). Further,
320 creatinine levels were within normal limits throughout the study, suggesting that there was no
321 detectable kidney damage in the nTAF cohort (Figure 4Q). Liver enzymes were monitored as
322 surrogate markers for health; aspartate aminotransferase (AST) (Figure 4R), and alanine
323 aminotransferase (ALT) (Figure 4S) measurements were within normal levels with respect to

324 baseline values pre-nTAF implantation. Metabolic panel, complete blood count and urinalysis
325 results were also within normal levels (Figure S3A-V, 4A-N, Table S1, Supporting Information).

326

327 **3. Discussion**

328 This work represents the first ever preventive efficacy assessment of an implantable LA ARV
329 platform and the foremost study of LA TAF as a single agent HIV PrEP regimen. Our finding
330 that nTAF protected from SHIV infection with 62.50% reduction in risk of infection per
331 exposure resembles that of TAF predecessor, tenofovir disoproxil fumarate (TDF). TDF
332 monotherapy resulted in 60.00% protective efficacy in macaques^[32], but clinically achieved 67%
333 risk reduction and 86.00% preventive efficacy in individuals with detectable plasma
334 tenofovir.^[5,33]

335

336 There is no benchmark preventive level of TFV-DP in PBMCs for sustained subcutaneous
337 administration of TAF. We used as a reference the TFV-DP concentration in PBMCs of 100
338 fmol/10⁶ cells, which conservatively exceeds the levels identified as protective in the iPrEX trial
339 with Truvada® (cryopreserved PBMC, 16.00 fmol/10⁶ cells; freshly lysed PBMC, 40.00
340 fmol/10⁶ cells).^[6] Other TAF-releasing implants are targeting 24-48 fmol/10⁶, a target that takes
341 into consideration the 66% TFV-DP loss during cryopreservation in the iPrEX trial.^[7,9,10] While
342 not directly comparable to oral Truvada administration, we used 100 fmol/10⁶ cells as rational
343 target to exceed prior to start the viral challenges. Nonetheless, this is the first efficacy study
344 with continuous TAF administration via the subcutaneous route. Our results show that by
345 maintaining a median TFV-DP concentration of 390 fmol/10⁶ PBMC (IQR, 216.50 to 585.50
346 fmol/10⁶ PBMC) we achieved partial protection with 62.50% efficacy (95% CI, 1.72% to

347 85.69%). In light of our studies, it remains unclear what the preventive benchmark could be to
348 establish 100% efficacy in a rectal challenge model.
349
350
351 Most clinical studies evaluating PrEP adherence use plasma, PBMC or dried blood spots as
352 surrogate markers to local tissue concentrations.^[5,6,33,34] However, breakthrough infection has
353 occurred in individuals with high systemic drug concentrations, similar to the infected nTAF
354 animals in our study. Therefore, it remains unclear if infection in some animals in our study
355 could be attributable to inadequate TFV-DP concentrations in the site of viral transmission. In a
356 study of weekly oral TAF as a single-agent PrEP against vaginal SHIV infection by the Center
357 for Disease Control, TFV-DP PBMC levels were similar between the four infected and five
358 uninfected animals.^[30] However, only five out of nine animals had detectable vaginal TFV-DP
359 concentrations (5 fmol/mg) prior to challenge.^[30] It is also of interest to identify the turn-over
360 rate of “TFV-DP positive” to “TFV-DP naïve” mononuclear cells systemically and locally at the
361 site of transmission to improve dosing regimens. Garcia-Lerma et. al demonstrated that once
362 weekly oral TAF dosing conferred low protection from HIV transmission, despite high systemic
363 (>1000 fmol/10⁶ PBMC) and rectal (median, 377 fmol/10⁶ mononuclear cells) TFV-DP
364 levels.^[35] However, in the aforementioned study the animals were rectally challenged 3 days
365 after the first weekly oral TAF dose. Thus, the long interval between drug dosing and virus
366 exposure could have allowed for TFV-DP naïve mononuclear cells to repopulate at the site of
367 transmission. Of relevance, on-demand local TFV delivery at HIV transmission sites, such as a
368 TFV rectal douche, has shown to achieve high local tissue concentrations and favorable PK
369 profiles in NHP with SHIV challenges.^[36,37] Therefore, we posit that PrEP efficacy could

370 plausibly be improved if first-line target cells have sufficient TFV-DP concentrations prior to
371 virus exposure.

372

373 The present study was limited by the number of animals and the use of both sexes for rectal
374 SHIV prevention. Future studies could address this issue by increasing the sample size and
375 conducting separate sexes studies to evaluate protection against rectal or vaginal exposure.
376 Further, because Descovy® is clinically approved for oral administration, scientific rigor could
377 be strengthened with an additional group with daily oral TAF dosing as opposed to weekly
378 dosing as performed in literature, in comparison to sustained subcutaneous delivery.

379

380 In summary, our innovative strategy of continuous low-dose systemic delivery of TAF obviates
381 adherence challenges and provides similar protective benefit to that observed with oral TDF.
382 Taken together, this work provides optimism for implementing clinical studies to assess the
383 safety and efficacy of LA TAF platforms for HIV PrEP.

384

385 **4. Experimental Section**

386

387 *Nanofluidic implant assembly*

388 Medical-grade 6Al4V titanium oval drug reservoirs were specifically designed and manufactured
389 for this study. Briefly, a nanofluidic membrane possessing 278,600 nanochannels (mean; 194
390 nm) was mounted on the inside of the sterile drug reservoir as described previously.^[12] Detailed
391 information regarding the membrane structure and fabrication was described previously.^[26,38]
392 Implants were welded together using Arc welding. PrEP implants were loaded with ~300 - 457

393 mg TAF fumarate using a funnel in the loading port, while control implants were left empty. A
394 titanium piece that resembled a small nail was inserted into the loading port and welded shut.
395 Implants were primed for drug release through the nanofluidic membrane by placing implants in
396 1 X Phosphate Buffered Saline (PBS) under vacuum. This preparation method resulted in
397 loading of control implants with PBS. Implants were maintained in sterile 1X PBS in a
398 hermetically sealed container until implantation shortly after preparation. TAF was kindly
399 provided by Gilead Sciences, Inc.

400

401 *In vitro release from nanofluidic implant*

402 In an effort to limit the amount of drug used, the in vitro release study was performed using
403 nanochannel membranes with identical structure and channel size those adopted in vivo, but with
404 a small number of nanochannels (n= 9,800 as compared to n=278,600 for the full-size
405 membrane). In vitro release results were then linearly scaled to account for the difference in
406 nanochannels number. Medical-grade 6Al4V titanium cylindrical drug reservoirs (n=5) were
407 assembled as described above, loaded with ~20.00 mg TAF fumarate and placed in sink solution
408 of 20 mL 1 × PBS with constant agitation at 37°C. For analysis, the entire sink solution was
409 retrieved and replaced with fresh PBS every other day for 20 days. The maximum TAF
410 concentration regarding TAF saturation in sink solution was <10%, therefore maintaining sink
411 condition. High-performance liquid chromatography (HPLC) analysis was performed on an
412 Agilent Infinity 1260 system equipped with a diode array and evaporative light scattering
413 detectors using a 3.5- μ m 4.6 × 100 mm Eclipse Plus C18 column and water/methanol as the
414 eluent and 25 μ L injection volume. Peak areas were analyzed at 260 nm absorbance.

415

416 *Nanofluidic membrane assessment*

417 Silicon nanofluidic membranes structure and composition was assessed using different imaging
418 techniques at the Microscopy – SEM/AFM core of the Houston Methodist Research Institute
419 (HMRI), Houston, TX, USA. Inspection of structural conformation was performed via scanning
420 electron microscopy (SEM; Nova NanoSEM 230, FEI, Oregon, USA), nanochannel dimension
421 was measured on membrane cross sections obtained using gallium ion milling (FIB, FEI 235).
422 Surface roughness was measured by atomic force microscopy (AFM Catalyst), surface chemical
423 composition was evaluated with Energy-dispersive X-ray spectroscopy (EDAX, Nova NanoSEM
424 230).

425

426 *Animals and animal care*

427 All animal procedures were conducted at the AAALAC-I accredited Michale E. Keeling Center
428 for Comparative Medicine and Research, The University of Texas MD Anderson Cancer Center
429 (UTMDACC), Bastrop, TX. All animal experiments were carried out according to the provisions
430 of the Animal Welfare Act, PHS Animal Welfare Policy, and the principles of the NIH Guide for
431 the Care and Use of Laboratory Animals. All procedures were approved by the Institutional
432 Animal Care and Use Committee (IACUC) at UTMDACC, which has an Animal Welfare
433 Assurance on file with the Office of Laboratory Animal Welfare. IACUC #00001749-RN00.
434 Indian rhesus macaques (*Macaca mulatta*; n=14; 6 males and 8 females) of 2-4 years and 2-5 kg
435 bred at this facility were used in the study. All procedures were performed under anesthesia with
436 ketamine (10 mg/kg, intramuscular) and phenytoin/pentobarbital (1 mL/10 lbs, intravenous
437 [IV]).

438

439 All animals had access to clean, fresh water at all times and a standard laboratory diet. Prior to
440 the initiation of virus inoculations, compatible macaques were pair-housed. Once inoculations
441 were initiated, the macaques were separated into single housing (while permitting eye contact) to
442 prevent the possibility of SHIV transmission between the macaques. Euthanasia of the macaques
443 was accomplished in a humane manner (IV pentobarbital) by techniques recommended by the
444 American Veterinary Medical Association Guidelines on Euthanasia. The senior medical
445 veterinarian verified successful euthanasia by the lack of a heartbeat and respiration.

446

447 *Minimally invasive implantation procedure*

448 An approximately 1-cm dorsal skin incision was made on the right lateral side of the thoracic
449 spine. Blunt dissection was used to make a subcutaneous pocket ventrally about 5 cm deep. The
450 implant was placed into the pocket with the membrane facing the body. A simple interrupted
451 tacking suture of 4-0 polydioxanone (PDS) was placed in the subcutaneous tissue to help close
452 the dead space and continued intradermally to close the skin. All animals received a single
453 50,000 U/kg perioperative penicillin G benzathine/penicillin G procaine (Combi-Pen) injection
454 and subcutaneous once-daily meloxicam (0.2 mg/kg on day 1 and 0.1 mg/kg on days 2 and 3) for
455 postsurgical pain.

456

457 *Blood collection and plasma and PBMC sample preparation*

458 All animals had weekly blood draws to assess plasma TAF and TFV concentrations, intracellular
459 TFV-DP PBMC concentrations, plasma viral RNA loads, and cell-associated SHIV DNA in
460 PBMCs. Blood collection and sample preparation were performed as previously described.^[11]
461 Blood was collected in EDTA-coated vacutainer tubes before implantation; on days 1, 2, 3, 7, 10,

462 and 14; and then once weekly until euthanasia. Plasma was separated from blood by
463 centrifugation at $1200 \times g$ for 10 min at $4 \text{ }^{\circ}\text{C}$ and stored at $-80 \text{ }^{\circ}\text{C}$ until analysis. The remaining
464 blood was used for PBMC separation by standard Ficoll-Hypaque centrifugation. Cell viability
465 was $> 95\%$. After cells were counted, they were pelleted by centrifugation at $400 \times g$ for 10 min,
466 resuspended in $500 \text{ }\mu\text{L}$ of cold 70% methanol/30% water, and stored at $-80 \text{ }^{\circ}\text{C}$ until further use.

467

468 *Pharmacokinetic analysis of TFV-DP in PBMC and TAF and TFV in plasma*

469 The PK profiles of TFV-DP in PBMC and TAF and TFV in plasma were evaluated throughout
470 the 4 months of nTAF implantation. Due to early implant removal in one animal on day 43,
471 seven animals were evaluated for drug PK. After device explantation, drug washout was assessed
472 for an additional 2 months (n=3).

473

474 Intracellular TFV-DP concentrations in PBMCs were quantified using previously described
475 validated liquid chromatographic-tandem mass spectrometric (LC-MS/MS) analysis.^[6,39] The
476 assay was linear from 5 to 6000 fmol/sample. Typically, 25 fmol/sample was used as the lower
477 limit of quantitation (LLOQ). If additional sensitivity was needed, standards and quality controls
478 were added down to 5 fmol/samples, as previously described.^[39] Day 21 TFV-DP concentrations
479 were omitted due to PBMC count below threshold.

480

481 Plasma TAF and TFV concentrations were quantified using a previously described LC-MS/MS
482 assay.^[40] Drugs were extracted from 0.1 mL plasma via solid phase extraction; assay lower limits
483 of quantitation for TAF and TFV were 0.03 ng/mL and 1 ng/mL, respectively. The multiplexed

484 assay was validated in accordance with FDA, Guidance for Industry: Bioanalytical Method

485 Validation recommendations.^[41]

486

487 *Tissue TFV-DP quantification*

488 Lymphoid tissues (mesenteric, axillary, and inguinal lymph nodes), rectum, urethra, cervix,

489 tonsil, spleen, and liver were homogenized, and 50- to 75-mg aliquots were used for TFV-DP

490 quantitation. Pharmacokinetic analysis of TFV-DP was conducted by the Clinical Pharmacology

491 Analytical Laboratory at the Johns Hopkins University School of Medicine. TFV concentrations

492 in aforementioned tissue biopsies were determined via LC-MS/MS analysis. TFV-DP was

493 measured using a previously described indirect approach, in which TFV was quantitated

494 following isolation of TFV-DP from homogenized tissue lysates and enzymatic conversion to the

495 TFV molecule.^[39] The assay LLOQ for TFV-DP in tissue was 5 fmol/sample, and drug

496 concentrations were normalized to the amount of tissue analyzed.^[42] The TFV-DP tissue was

497 validated in luminal tissue (rectal and vaginal tissue) in accordance with FDA, Guidance for

498 Industry: Bioanalytical Method Validation recommendations^[41]; alternative tissue types were

499 analyzed using this method.

500

501 *PrEP nTAF efficacy against rectal SHIV challenge*

502 To study the efficacy of the PrEP implant against SHIV transmission, animals were divided into

503 two groups, PrEP nTAF-treated [n=8; 4 male (M) and 4 female (F)] or control nPBS (n=6; 3 M

504 and 3 F), in a non-blinded study. The PrEP regimen consisted of subcutaneously implanted

505 nTAF for sustained drug release over 112 days. The efficacy of nTAF in preventing rectal SHIV

506 transmission was evaluated using a repeat low-dose exposure model described previously.^[32,35,43]

507 Animals were considered protected if they remained negative for SHIV RNA throughout the
508 study. Briefly, after PrEP-treated macaques achieved intracellular TFV-DP concentrations above
509 100.00 fmol/10⁶ PBMCs, both groups were rectally exposed to SHIV_{SF162P3} once a week for up
510 to 10 weeks until infection was confirmed by two consecutive positive plasma viral RNA loads.
511 The SHIV_{SF162P3} dose was in range of HIV-1 RNA levels found in human semen during acute
512 viremia.^[43]

513
514 Challenge stocks of SHIV_{162p3} were generously supplied by Dr. Nancy Miller, Division of AIDS,
515 NIAID, through Quality Biological (QBI), under Contract No. HHSN272201100023C to the
516 Vaccine Research Program, Division of AIDS, NIAID. The stock SHIV_{162p3} R922 derived
517 harvest 4 dated 9/16/2016 (p27 content 173.33 ng/ml, viral RNA load >10⁹ copies/ml,
518 TCID50/ml in rhesus PBMC 1280) was diluted 1:300 and 1ml of virus was used for rectal
519 challenge each time.

520
521 For the challenge, the animals were positioned in prone position and virus was inoculated
522 approximately 4 cm into the rectum. Inoculated animals were maintained in the prone position
523 with the perineum elevated for 20 minutes to ensure that virus did not leak out. Care was also
524 taken to prevent any virus from contacting the vagina area and to not abrade the mucosal surface
525 of the rectum.

526
527 *Infection monitoring by SHIV RNA in plasma and SHIV DNA in tissues*

528 Infection was monitored by the detection of SHIV RNA in plasma using previously described
529 methods^[44,45] with modification. Viral RNA (vRNA) was isolated from blood plasma using the

530 Qiagen QIAmp UltraSense Virus Kit (Qiagen #53704) in accordance with manufacturer's
531 instructions for 0.5 mL of plasma. vRNA levels were determined by quantitative real-time PCR
532 (qRT-PCR) using Applied Biosystems™ TaqMan™ Fast Virus 1-Step Master Mix
533 (Thermofisher #4444432) and a primer-probe combination recognizing a conserved region of
534 gag (GAG5f: 5'-ACTTTCGGTCTTAGCTCCATTAGTG-3'; GAG3r: 5'-
535 TTTTGCTTCCTCAGTGTGTTTCA-3'; and GAG1tq: FAM 5'-
536 TTCTCTTCTGCGTGAATGCACCAGATGA-3'TAMRA). Each 20 µl reaction contained 900
537 nM of each primer and 250 nM of probe, and 1x Fast Virus 1-Step Master Mix, plasma-derived
538 vRNA sample, SIV gag RNA transcript containing standard, or no template control.
539
540 qRT-PCR was performed in a ABI Step One Plus Cyclor. PCR was performed with an initial
541 step at 50°C for 5 min followed by a second step at 95°C for 20 sec, and then 40 cycles of 95°C
542 for 15 sec and 60°C for 1 min. Ten-fold serial dilutions (1 to 1 x 10⁶ copies per reaction) of an in
543 vitro transcribed SIV gag RNA were used to generate standard curves. Each sample was tested
544 in duplicate reactions. Plasma viral loads were calculated and shown as viral RNA copies/mL
545 plasma. The limit of detection is 50 copies/ml. Infections were confirmed after a consecutive
546 positive plasma viral load measurement.
547
548 To detect viral DNA in tissue samples, total DNA was isolated from PBMCs or tissue specimens
549 using the Qiagen DNeasy Blood & Tissue Kit (Qiagen #69504) according to the manufacturer's
550 protocol. DNA was quantified using a nanodrop spectrophotometer. qRT-PCR was performed
551 using the SIV gag primer probe set described above. Each 20 µl reaction contained 900 nM of
552 each primer and 250 nM of probe, and 1x TaqMan Gene Expression Master Mix (Applied

553 Biosystems, Foster City, CA), macaque-derived DNA sample, SIV gag DNA containing
554 standard, or no template control. PCR was initiated in with an initial step of 50°C for 2 min and
555 then 95°C for 10 min. This was followed by 40 cycles of 95°C for 15 sec, and 60°C for 1 min.
556 Each sample was tested in triplicate reactions. Ten-fold serial dilutions of a SIV gag DNA
557 template (1 to 1 x 10⁵ per reaction) were used to generate standard curves. The limit of detection
558 of this assay was determined to be 1 copy of SIV gag DNA.

559

560 *Device retrieval and macaque euthanasia*

561 A subset of PrEP-treated macaques (n=4), those with the highest viral load, were euthanized on
562 day 112, while implants were retrieved on day 112 from the remaining PrEP-treated macaques
563 (n=3) for continuation to a 2-month drug-washout period before euthanasia. SHIV-infected
564 macaques in the control group (n=6) were transferred to another study (data not shown) and
565 euthanized 28 days later. The implant was retrieved with a small incision in the skin and stored at
566 -80 °C until further analysis. Skin within a 2-cm margin surrounding the implant was excised
567 from euthanized macaques and fixed in 10% buffered formalin for histological analysis.
568 Macaques continuing in the washout period underwent a skin punch biopsy of the subcutaneous
569 pocket, and the skin incision was sutured with a simple interrupted tacking suture of 4-0 PDS;
570 the specimen was fixed in 10% buffered formalin for histological analysis. The following tissues
571 were collected from all animals at euthanasia (n=13): lymphoid tissues (mesenteric, axillary, and
572 inguinal lymph nodes), rectum, urethra, cervix, tonsil, spleen, and liver. Tissues were snap-
573 frozen and stored at -80 °C until further analysis of TAF concentrations, viral RNA loads, and
574 cell-associated SHIV DNA.

575

576 *Residual drug and nanofluidic membrane retrieval from explanted implants*

577 Upon explantation, the implants were snap frozen with liquid nitrogen to preserve residual drug
578 for stability analysis. For residual drug retrieval, the implants were thawed at 4°C overnight. A
579 hole was drilled on the outermost corner on the back of the implant using a 3/64 titanium drill bit
580 with a stopper. Drilling was performed on the back of the implant and distal to the membrane to
581 avoid damage. Following drilling, 20 µL sample from the implant drug reservoir was aliquoted
582 into respective 1.5 mL Eppendorf tubes with 0.5 mL 100% ethanol using a pipette. The implants
583 were placed in 50 mL conical tubes with 40.0 g 70% ethanol. Each implant was flushed using a
584 19-gauge needle with 70% ethanol from the sink solution. For sterilization, the implants were
585 incubated in 70% ethanol for 4 days and transferred to new conical tubes with fresh 70% ethanol
586 for an additional 4 days. To ensure nanochannel membranes were dry, the implants were
587 transferred to new conical tubes with 100% ethanol for a day and placed in 6-well plates to dry
588 under vacuum. To protect the membrane during machining procedure, electrical tape was placed
589 over the outlets. The implants were opened using a rotary tool with a diamond wheel. Titanium
590 dust from machining procedure was gently cleaned from membrane with a cotton swab and 70%
591 ethanol. To remove membrane from the implant, a drop of nitric acid (Trace Metal grade) was
592 placed on the membrane overnight and rinsed with Millipore water the next day. Membranes
593 were kept in hermetically sealed containers until analysis.

594

595 *TAF stability analysis in drug reservoir*

596 Liquid in the drug reservoir after explantation was collected with a pipette and diluted 25 times
597 with 100% ethanol. The samples were transferred to 0.2 µm nylon centrifugal filters and
598 centrifuged at 500 G for 8 minutes at room temperature. An aliquot of 50 µL from the filtered

599 samples were further diluted in 100 μ L 100% ethanol. HPLC analysis was performed on an
600 Agilent Infinity 1260 system equipped with a diode array and evaporative light scattering
601 detectors using a 3.5- μ m 4.6 \times 100 mm Eclipse Plus C18 column and water/methanol as the
602 eluent and 25 μ L injection volume. Peak areas were analyzed at 260 nm absorbance.

603
604 Drug solids from within the implant were analyzed from the initial 40.0 g 70% ethanol sink
605 solution. The samples were transferred to 0.2 μ m nylon centrifugal filter and centrifuged at 500
606 G for 8 minutes at room temperature. An aliquot of 10 μ L from the filtered samples was further
607 diluted in 990 μ L of deionized water. UV-vis spectroscopy was performed on a Beckman
608 Coulter DU® 730 system. Peak areas were analyzed at 260 nm absorbance.

609
610 *Assessment of PrEP nTAF safety and tolerability*

611 Tissues were fixed in 10% buffered formalin and stored in 70% ethanol until analysis. Tissues
612 were then embedded in paraffin, cut into 5 μ m sections and stained with hematoxylin and eosin
613 (H&E) staining at the Research Pathology Core HMRI, Houston, TX, USA. H&E staining was
614 performed on tissue sections surrounding the implant site and kidney. Histological assessment
615 was performed by a blinded pathologist. For immunohistochemistry evaluation of tissue
616 sections, slides were stained with anti-CD45 conjugated to fluorescein isothiocyanate
617 (Pharmingen). For negative controls, corresponding immunoglobulin and species (IgG)-matched
618 isotype control antibodies were used. Nonspecific binding in sections was blocked by a 1-hour
619 treatment in tris-buffered saline (TBS) plus 0.1% w/v Tween containing defatted milk powder
620 (30 mg ml⁻¹). Stained sections were mounted in Slow Fade GOLD with 4',6-diamidino-2-
621 phenylindole (DAPI) (Molecular Probes, OR) and observed using a Nikon T300 Inverted

622 Fluorescent microscope (Nikon Corp., Melville, NY). For verification of cell phenotype, each
623 slide was scored by counting three replicate measurements by the same observer for each slide.
624 All slides were counted without knowledge of the cell-specific marker being examined, and
625 results were confirmed through a second reading by another observer.

626

627 *Assessment of TAF toxicity*

628 To assess TAF toxicity, a comprehensive metabolic panel was analyzed for each animal weekly
629 during the rectal challenge phase of the study and biweekly afterward. Urine and CBCs were
630 analyzed monthly to assess kidney and liver function and monitor the well-being of the NHPs.

631

632 *Statistical analysis*

633 Plasma $t_{1/2}$ PK analysis was performed in Microsoft Excel using 2 time points, days 112 and 119.
634 Results were expressed as actual $t_{1/2}$ is less than obtained $t_{1/2}$ (because day 119 values were
635 undetectable and were substituted with BLOQ values). PBMC PK analysis was performed using
636 PKSolver add-in for Microsoft Excel developed by Zhang et al.^[46] Data are represented as mean
637 \pm SD or median with interquartile range (IQR) between the first (25th percentile) and third (75th
638 percentile) quartiles. The relative risk and relative risk reduction with 95% confidence intervals
639 (95% CI) were estimated to examine the per-exposure effect of TAF, and the Fisher's exact was
640 used for the comparison. The Mann-Whitney test was used to compare the median survival time
641 and the differences in SHIV RNA levels at initial detection. The Kaplan-Meier analysis was
642 performed between the PrEP and control groups, with the use of the number of inoculations as
643 the time variable. The exact log-rank test was used to test the survival between the two groups.
644 All statistical analysis for calculation of the efficacy of TAF were performed with GraphPad

645 Prism 8 (version 8.2.0; GraphPad Software, Inc., La Jolla, CA). Statistical significance was
646 defined as two-tailed $p < 0.05$ for all tests.

647

648 **Supporting Information**

649 Supporting Information is available from the Wiley Online Library or from the author.

650

651 **Acknowledgements**

652 We thank Dr. Andreana L. Rivera, Yuelan Ren, and Sandra Steptoe from the research pathology
653 core of Houston Methodist Research Institute. Dr. Jianhua “James” Gu from the electron
654 microscopy core. We thank Simone Capuani from the Houston Methodist Research Institute for
655 implant design and rendering, Dixita Viswanath for help with tissue dissection, and Nicola Di
656 Trani for obtaining FIB image. We thank Dr. Dorothy Lewis for the useful discussions. We
657 thank Luke Segura, Elizabeth Lindemann and Dr. Greg Wilkerson from the Michale E. Keeling
658 Center for Comparative medicine and Research at UTMDACC for support in animal studies and
659 Bharti Nehete for plasma and PBMC isolation and virus challenge preparation. TAF fumarate
660 was provided by Gilead Sciences, Inc. **Funding:** This work was supported by funding from the
661 National Institutes of Health National Institute of Allergy and Infectious Diseases
662 (R01AI120749; A.G.), the National Institutes of Health National Institute of General Medical
663 Sciences (R01GM127558; A.G.) and Gilead Sciences (A.G.). F.P.P. received funding support
664 from Tecnologico de Monterrey and Consejo Nacional de Ciencia y Tecnologia.

665

666

667 References

- 668 [1] UNAIDS, “90-90-90 An ambitious treatment target to help end the AIDS epidemic,”
669 **2014**.
- 670 [2] A. S. Ray, M. W. Fordyce, M. J. M. Hitchcock, *Antiviral Res.* **2016**, *125*, 63.
- 671 [3] R. M. Grant, J. R. Lama, P. L. Anderson, V. McMahan, A. Y. Liu, L. Vargas, P.
672 Goicochea, M. Casapía, J. V. Guanira-Carranza, M. E. Ramirez-Cardich, et al., *N. Engl. J. Med.*
673 **2010**, *363*, 2587.
- 674 [4] M. S. Cohen, Y. Q. Chen, M. McCauley, T. Gamble, M. C. Hosseinipour, N.
675 Kumarasamy, J. G. Hakim, J. Kumwenda, B. Grinsztejn, J. H. S. Pilotto, et al., *N. Engl. J. Med.*
676 **2011**, *365*, 493.
- 677 [5] J. M. Baeten, D. Donnell, P. Ndase, N. R. Mugo, J. D. Campbell, J. Wangisi, J. W.
678 Tappero, E. A. Bukusi, C. R. Cohen, E. Katabira, et al., *N. Engl. J. Med.* **2012**, *367*, 399.
- 679 [6] P. L. Anderson, D. V Glidden, A. Liu, S. Buchbinder, J. R. Lama, J. V. Guanira, V.
680 McMahan, L. R. Bushman, M. Casapia, O. Montoya-Herrera, et al., *Sci. Transl. Med.* **2012**, *4*,
681 151ra125.
- 682 [7] M. Gunawardana, M. Remedios-Chan, C. S. Miller, R. Fanter, F. Yang, M. A. Marzinke,
683 C. W. Hendrix, M. Beliveau, J. A. Moss, T. J. Smith, *Antimicrob. Agents Chemother.* **2015**,
684 AAC.
- 685 [8] E. Schlesinger, D. Johengen, E. Luecke, G. Rothrock, I. McGowan, A. van der Straten, T.
686 Desai, *Pharm. Res.* **2016**, *33*, 1649.
- 687 [9] L. M. Johnson, S. A. Krovi, L. Li, N. Girouard, Z. R. Demkovich, D. Myers, B.
688 Creelman, A. van der Straten, *Pharmaceutics* **2019**, *11*, 315.
- 689 [10] J. T. Su, S. M. Simpson, S. Sung, E. Bryndza Tfaily, R. Veazey, M. Marzinke, J. Qiu, D.

- 690 Watrous, L. Widanapathirana, E. Pearson, et al., *Antimicrob. Agents Chemother.* **2019**, DOI
691 10.1128/AAC.01893-19.
- 692 [11] C. Y. X. Chua, P. Jain, A. Ballerini, G. Bruno, R. L. Hood, M. Gupte, S. Gao, N. Di
693 Trani, A. Susnjar, K. Shelton, et al., *J. Control. Release* **2018**, 286, 315.
- 694 [12] F. P. Pons-Faudoa, A. Sizovs, N. Di Trani, J. Paez-Mayorga, G. Bruno, J. Rhudy, M.
695 Manohar, K. Gwenden, C. Martini, C. Y. X. Chua, et al., *J. Control. Release* **2019**, 306, 89.
- 696 [13] M. A. Boyd, D. A. Cooper, *Lancet* **2017**, 390, 1468.
- 697 [14] M. E. Clement, R. Kofron, R. J. Landovitz, *Curr. Opin. HIV AIDS* **2020**, 15, 19.
- 698 [15] Intarcia Therapeutics, “Medici System Pipeline,” can be found under
699 <https://www.intarcia.com/pipeline-technology/itca-650.html>, **n.d.**
- 700 [16] F. P. Pons-Faudoa, A. Ballerini, J. Sakamoto, A. Grattoni, *Biomed. Microdevices* **2019**,
701 21, 47.
- 702 [17] C. Flexner, *Curr. Opin. HIV AIDS* **2018**, 13, 374.
- 703 [18] M. Markowitz, I. Frank, R. M. Grant, K. H. Mayer, R. Elion, D. Goldstein, C. Fisher, M.
704 E. Sobieszczyk, J. E. Gallant, H. Van Tieu, et al., *Lancet HIV* **2017**, 4, e331.
- 705 [19] R. J. Landovitz, S. Li, B. Grinsztejn, H. Dawood, A. Y. Liu, M. Magnus, M. C.
706 Hosseinipour, R. Panchia, L. Cottle, G. Chau, et al., *PLOS Med.* **2018**, 15, e1002690.
- 707 [20] Merck & Co., “Press Release Details,” can be found under
708 [https://investors.merck.com/news/press-release-details/2019/Merck-Presents-Early-Evidence-on-](https://investors.merck.com/news/press-release-details/2019/Merck-Presents-Early-Evidence-on-Extended-Delivery-of-Investigational-Anti-HIV-1-Agent-Islatravir-MK-8591-via-Subdermal-Implant/default.aspx)
709 [Extended-Delivery-of-Investigational-Anti-HIV-1-Agent-Islatravir-MK-8591-via-Subdermal-](https://investors.merck.com/news/press-release-details/2019/Merck-Presents-Early-Evidence-on-Extended-Delivery-of-Investigational-Anti-HIV-1-Agent-Islatravir-MK-8591-via-Subdermal-Implant/default.aspx)
710 [Implant/default.aspx](https://investors.merck.com/news/press-release-details/2019/Merck-Presents-Early-Evidence-on-Extended-Delivery-of-Investigational-Anti-HIV-1-Agent-Islatravir-MK-8591-via-Subdermal-Implant/default.aspx), **2019**.
- 711 [21] *Gated Nanofluidic Valve For Active And Passive Electrosteric Control Of Molecular*
712 *Transport, And Methods Of Fabrication, U.S. Provisional Pat. Ser. No. 62/961,437, Filed Jan*

- 713 15. (2020), **2020**.
- 714 [22] A. Oliveros, A. Guiseppi-Elie, S. E. Sadow, *Biomed. Microdevices* **2013**, *15*, 353.
- 715 [23] C. A. Zorman, A. Eldridge, J. G. Du, M. Johnston, A. Dubnisheva, S. Manley, W. Fissell,
716 A. Fleischman, S. Roy, *Mater. Sci. Forum* **2012**, *717–720*, 537.
- 717 [24] N. Di Trani, A. Pimpinelli, A. Grattoni, *ACS Appl. Mater. Interfaces* **2020**, *12*, 12246.
- 718 [25] G. Bruno, N. Di Trani, R. L. Hood, E. Zabre, C. S. Filgueira, G. Canavese, P. Jain, Z.
719 Smith, D. Demarchi, S. Hosali, et al., *Nat. Commun.* **2018**, *9*, 1682.
- 720 [26] S. Ferrati, D. Fine, J. You, E. De Rosa, L. Hudson, E. Zabre, S. Hosali, L. Zhang, C.
721 Hickman, S. Sunder Bansal, et al., *J. Control. Release* **2013**, *172*, 1011.
- 722 [27] N. Di Trani, P. Jain, C. Y. X. Chua, J. S. Ho, G. Bruno, A. Susnjar, F. P. Pons-Faudoa, A.
723 Sizovs, R. L. Hood, Z. W. Smith, et al., *Nanomedicine Nanotechnology, Biol. Med.* **2019**, *16*, 1.
- 724 [28] N. Di Trani, A. Silvestri, G. Bruno, T. Geninatti, C. Y. X. Chua, A. Gilbert, G. Rizzo, C.
725 S. Filgueira, D. Demarchi, A. Grattoni, *Lab Chip* **2019**, *19*, 2192.
- 726 [29] A. Sizovs, F. P. Pons-faudoa, G. Malgir, K. A. Shelton, L. R. Bushman, C. Ying, X.
727 Chua, P. L. Anderson, P. N. Nehete, *Int. J. Pharm.* **2020**, *587*, 119623.
- 728 [30] I. Massud, M.-E. Cong, S. Ruone, A. Holder, C. Dinh, K. Nishiura, G. Khalil, Y. Pan, J.
729 Lipscomb, R. Johnson, et al., *J. Infect. Dis.* **2019**, *220*, 1826.
- 730 [31] P. L. Anderson, J. G. García-Lerma, W. Heneine, *Curr. Opin. HIV AIDS* **2016**, *11*, 94.
- 731 [32] S. Subbarao, R. A. Otten, A. Ramos, C. Kim, E. Jackson, M. Monsour, D. R. Adams, S.
732 Bashirian, J. Johnson, V. Soriano, et al., *J. Infect. Dis.* **2006**, *194*, 904.
- 733 [33] J. M. Baeten, D. Donnell, N. R. Mugo, P. Ndase, K. K. Thomas, J. D. Campbell, J.
734 Wangisi, J. W. Tappero, E. A. Bukusi, C. R. Cohen, et al., *Lancet Infect. Dis.* **2014**, *14*, 1055.
- 735 [34] P. L. Anderson, A. Y. Liu, J. R. Castillo-Mancilla, E. M. Gardner, S. M. Seifert, C.

- 736 McHugh, T. Wagner, K. Campbell, M. Morrow, M. Ibrahim, et al., *Antimicrob. Agents*
737 *Chemother.* **2017**, *62*, 1710.
- 738 [35] J. G. Garcia-Lerma, W. Aung, M. -e. Cong, Q. Zheng, A. S. Youngpairoj, J. Mitchell, A.
739 Holder, A. Martin, S. Kuklennyik, W. Luo, et al., *J. Virol.* **2011**, *85*, 6610.
- 740 [36] P. Xiao, S. Gumber, M. A. Marzinke, A. A. Date, T. Hoang, J. Hanes, L. M. Ensign, L.
741 Wang, L. Rohan, E. J. Fuchs, et al., *Antimicrob. Agents Chemother.* **2017**, *62*, DOI
742 10.1128/AAC.01644-17.
- 743 [37] E. Weld, E. Fuchs, M. Marzinke, “Conference Reports for NATAP: Tenofovir Rectal
744 Douche Provides Protective Drug Levels in MSM Colon Tissue - on-demand, behaviorally-
745 congruent,” can be found under http://www.natap.org/2018/HIVR4P/HIVR4P_26.htm, **2018**.
- 746 [38] D. Fine, A. Grattoni, S. Hosali, A. Ziemys, E. De Rosa, J. Gill, R. Medema, L. Hudson,
747 M. Kojic, M. Milosevic, et al., *Lab Chip* **2010**, *10*, 3074.
- 748 [39] L. R. Bushman, J. J. Kiser, J. E. Rower, B. Klein, J.-H. Zheng, M. L. Ray, P. L.
749 Anderson, *J. Pharm. Biomed. Anal.* **2011**, *56*, 390.
- 750 [40] P. Hummert, T. L. Parsons, L. M. Ensign, T. Hoang, M. A. Marzinke, *J. Pharm. Biomed.*
751 *Anal.* **2018**, *152*, 248.
- 752 [41] U.S. Department of Health and Human Services Food and Drug Administration, Center
753 for Drug Evaluation and Research (CDER), Center for Veterinary Medicine (CVM), *Guidance*
754 *for Industry: Bioanalytical Method Validation*, FDA, Rockville, MD, **2018**.
- 755 [42] E. Shieh, M. A. Marzinke, E. J. Fuchs, A. Hamlin, R. Bakshi, W. Aung, J. Breakey, T.
756 Poteat, T. Brown, N. N. Bumpus, et al., *J. Int. AIDS Soc.* **2019**, *22*, DOI 10.1002/jia2.25405.
- 757 [43] J. G. García-Lerma, R. A. Otten, S. H. Qari, E. Jackson, M. Cong, S. Masciotra, W. Luo,
758 C. Kim, D. R. Adams, M. Monsour, et al., *PLoS Med.* **2008**, *5*, e28.

- 759 [44] T. Biesinger, R. White, M. T. Yu Kimata, B. K. Wilson, J. S. Allan, J. T. Kimata,
760 *Retrovirology* **2010**, 7, 88.
- 761 [45] P. Polacino, B. Cleveland, Y. Zhu, J. T. Kimata, J. Overbaugh, D. Anderson, S.-L. Hu, J.
762 *Med. Primatol.* **2007**, 36, 254.
- 763 [46] Y. Zhang, M. Huo, J. Zhou, S. Xie, *Comput. Methods Programs Biomed.* **2010**, 99, 306.

764

765 **Author contributions**

766 **Fernanda P. Pons-Faudoa**: conceptualization, formal analysis, investigation, writing-original
767 draft preparation, writing-review and editing, visualization, project administration. **Antons**
768 **Sizovs**: conceptualization, methodology, formal analysis, investigation, writing-review and
769 editing, visualization. **Kathryn A. Shelton**: investigation. **Zoha Momin**: investigation. **Lane R.**
770 **Bushman**: methodology, validation, investigation. **Jiaqiong Xu**: formal analysis. **Corrine Y.**
771 **X. Chua**: formal analysis, writing-review and editing. **Joan E. Nichols**: methodology,
772 investigation, resources, writing-reviewing and editing. **Trevor Hawkins**: conceptualization,
773 writing-review and editing. **James F. Rooney**: conceptualization, writing-review and editing.
774 **Mark A. Marzinke**: methodology, validation, investigation, resources, data curation, writing-
775 review and editing. **Jason T. Kimata**: validation, investigation, resources, writing-review and
776 editing. **Peter L. Anderson**: methodology, validation, resources, writing-review and editing.
777 **Pramod N. Nehete**: investigation, resources, project administration, writing-review and editing.
778 **Roberto C. Arduino**: conceptualization, writing-review and editing. **Mauro Ferrari**: writing-
779 review and editing. **K. Jagannadha Sastry**: conceptualization, resources, writing-review and
780 editing. **Alessandro Grattoni**: conceptualization, investigation, resources, writing-original draft

781 preparation, writing-review and editing, visualization, supervision, project administration,
782 funding acquisition.

783

784 **Competing interests**

785 Study drugs were provided by Gilead Sciences. P.L.A. receives grants and contracts from Gilead

786 Sciences paid to his institution and collects personal fees from Gilead Sciences. T.H. is an

787 employee of Gilead Sciences. J.F.R. is an employee and stockholder of Gilead Sciences. All

788 other authors declare that they have no competing interests.

789

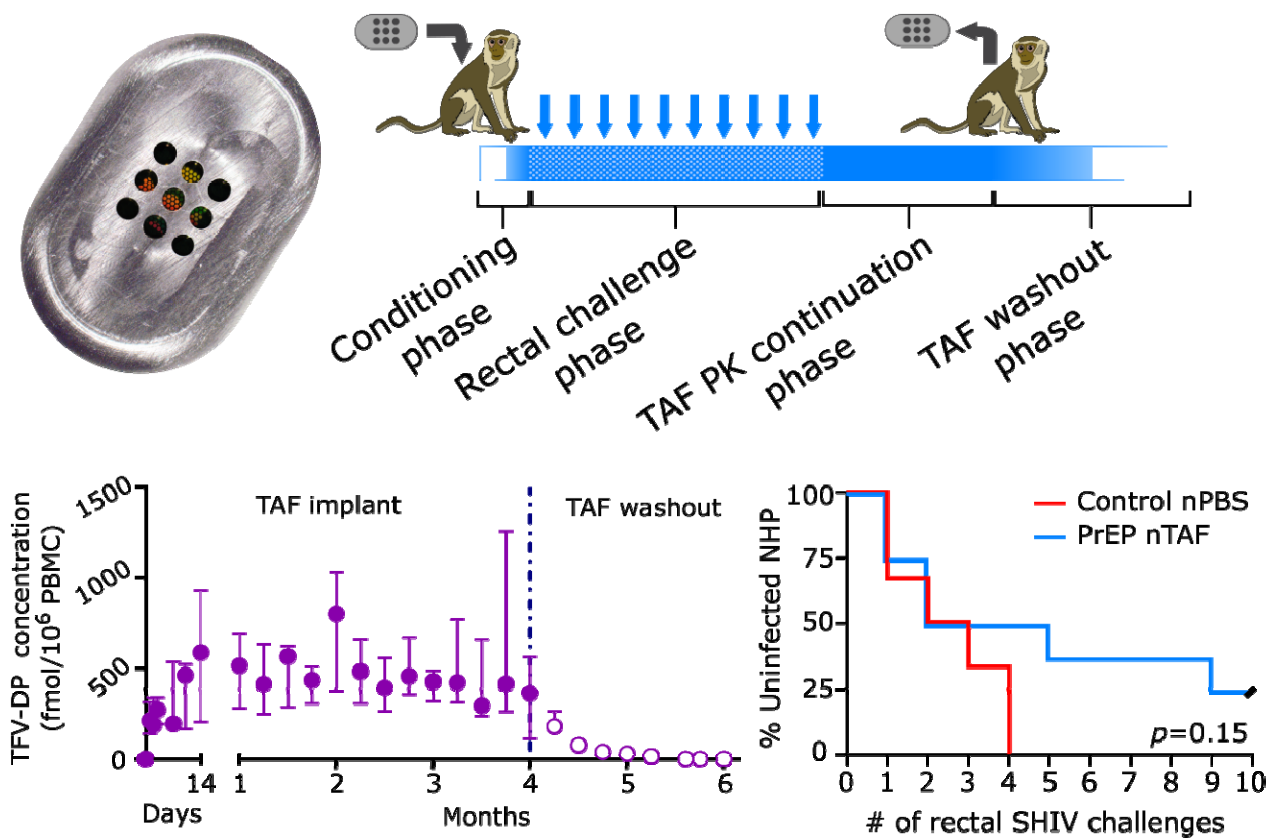
790 **Correspondence and requests for materials** should be addressed to A.G.

791 **Table of Contents (ToC)**

792 **ToC text:**

793 The Grattoni group performed the first HIV pre-exposure prophylaxis (PrEP) assessment of an
794 implantable long-acting antiretroviral platform. In this foremost study, the partial protection of
795 simian HIV with tenofovir alafenamide (TAF) delivered by a nanofluidic implant was
796 demonstrated in nonhuman primates.

797 **ToC figure:**



798

799

800 Supporting Information

801

802 Preventive efficacy of a tenofovir alafenamide fumarate nanofluidic implant in SHIV-

803 challenged nonhuman primates

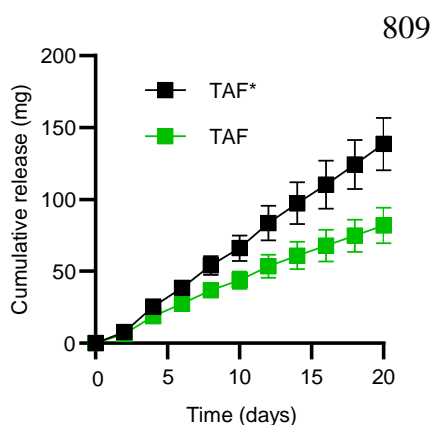
804 *Fernanda P. Pons-Faudoa*^{1,2}, *Antons Sizovs*¹, *Kathryn A. Shelton*³, *Zoha Momin*⁴, *Lane R.*

805 *Bushman*⁵, *Jiaqiong Xu*^{6,7}, *Corrine Ying Xuan Chua*¹, *Joan E. Nichols*⁸, *Trevor Hawkins*⁹, *James*

806 *F. Rooney*⁹, *Mark A. Marzinke*¹⁰, *Jason T. Kimata*⁴, *Peter L. Anderson*⁴, *Pramod N. Nehete*^{3,11},

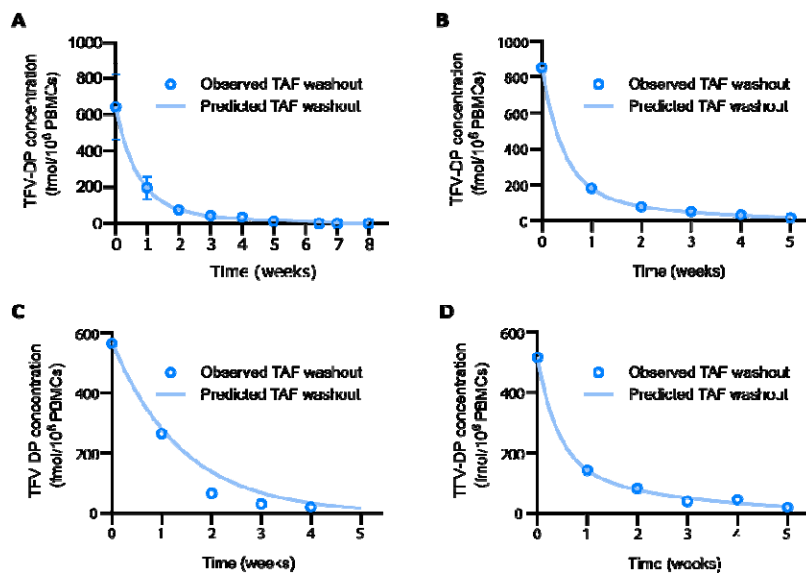
807 *Roberto C. Arduino*¹², *Mauro Ferrari*¹³, *K. Jagannadha Sastry*^{3,14}, *Alessandro Grattoni*^{1,15,16*}

808



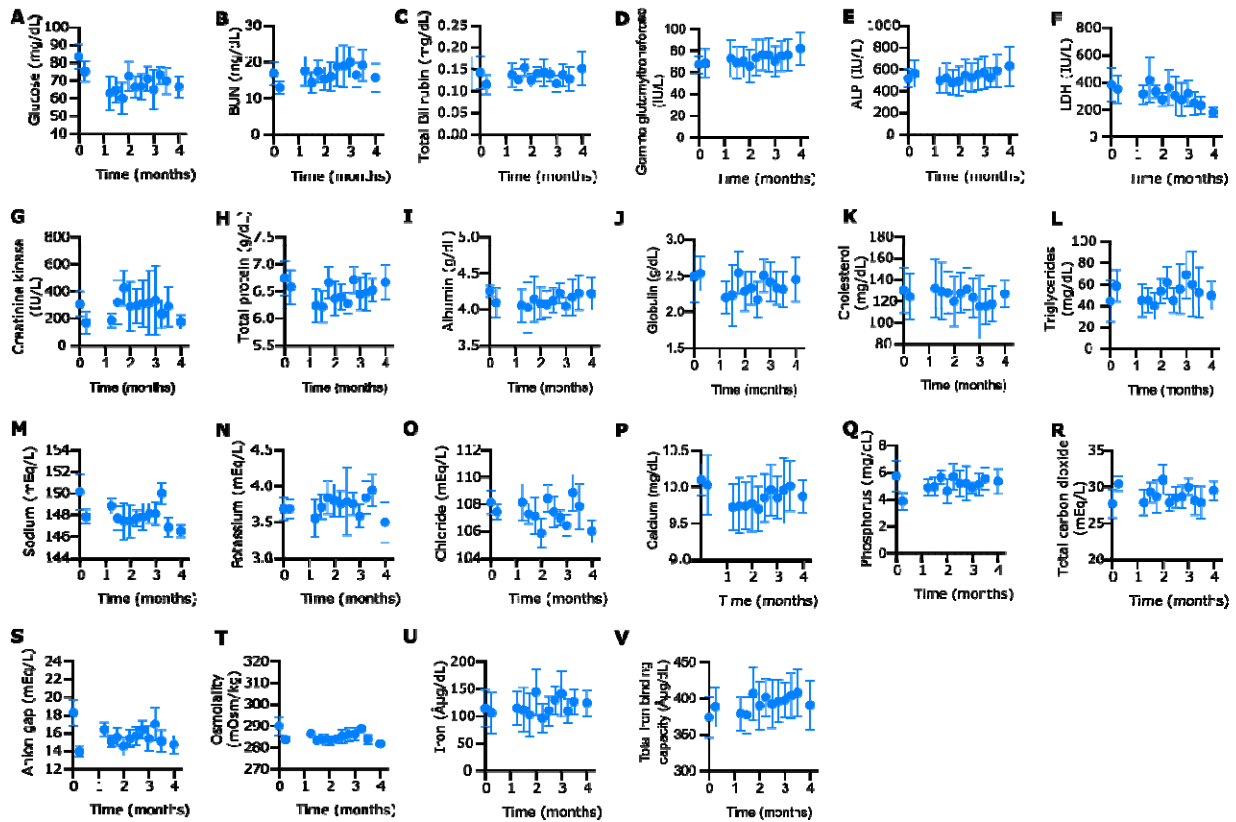
810 **Supporting Figure S1.** Cumulative in vitro release of TAF from nTAF (n=5). Sum of TAF*

811 shown in black. Data presented as mean \pm SEM.



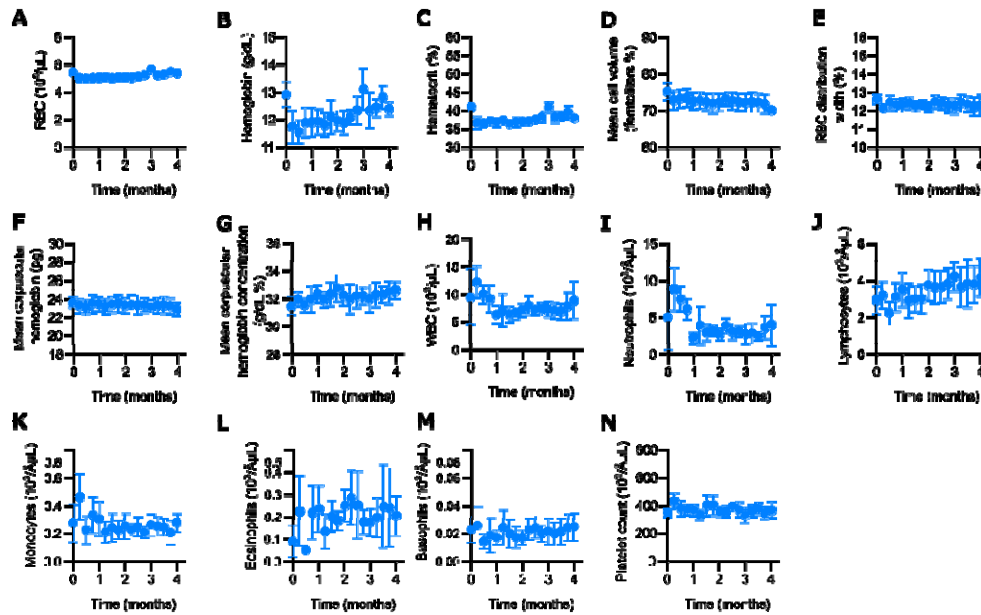
812

813 **Supporting Figure S2.** (A) nTAF TFV-DP washout fitted to intravenous bolus injection two-
814 compartment model to determine elimination rate constant. Data are presented as mean \pm SD.
815 (B) PrEP 5 nTAF TFV-DP washout fitted to intravenous bolus injection two-compartment model
816 to determine elimination rate constant. (C) PrEP 6 nTAF TFV-DP washout fitted to intravenous
817 bolus injection two-compartment model to determine elimination rate constant. (D) PrEP 7
818 nTAF TFV-DP washout fitted to intravenous bolus injection two-compartment model to
819 determine elimination rate constant.



820

821 **Supporting Figure S3.** Metabolic panel of rhesus macaques with nTAF. Baseline value for
822 comparison is on day 0 pre-implantation. All data presented as mean \pm SD.



823

824 **Supporting Figure S4.** CBC of rhesus macaques with nTAF. Baseline value for comparison is
825 on day 0 pre-implantation. All data presented as mean \pm SD.

826

827 **Supporting Table S1.** Urinalysis results in rhesus macaques with nTAF. Found in Excel File
828 named: Supporting Table S1.